Applied Catalysis B: Environmental 90 (2009) 526–534

Contents lists available at ScienceDirect

Applied Catalysis B: Environmental

journal homepage: www.elsevier.com/locate/apcatb

TiO_2/H_2O_2 mediated photocatalytic transformation of UV filter 4-methylbenzylidene camphor (4-MBC) in aqueous phase: Statistical optimization and photoproduct analysis

V.A. Sakkas [a], P. Calza [b,*], M. Azharul Islam [a], C. Medana [b], C. Baiocchi [b], K. Panagiotou [a], T. Albanis [a]

[a] Department of Chemistry, University of Ioannina, Ioannina 45110, Greece
[b] Dipartimento di Chimica Analitica, Università di Torino, via P. Giuria 5, 10125 Torino, Italy

ARTICLE INFO

Article history:
Received 12 January 2009
Received in revised form 3 April 2009
Accepted 9 April 2009
Available online 17 April 2009

Keywords:
Photocatalysis
TiO_2
Experimental design
Mineralization
Toxicity
UV filter

ABSTRACT

Central composite design (CCD) based on response surface methodology (RSM) was employed in the present study in combination with "profiling and desirability function" to evaluate the effects of main variables (TiO_2, H_2O_2, and light intensity) affecting 4-methylbenzylidene camphor (4-MBC) photocatalytic degradation and for optimization of the process.

Besides statistical optimization of the UV filter decomposition, the investigation involved a study of the identification of intermediate compounds, mineralization, as well as toxicity evaluation. The transformation of 4-MBC proceeds through: (i) demethylation of the bridged structure; (ii) hydroxylation of the methylbenzylidene moiety; (iii) bihydroxylation/demethylation reaction. Even if all the identified compounds are degraded themselves within 30 min, the complete carbon mineralization is only achieved after 24 h of irradiation. Toxicity assays using *Vibrio fischeri*, have shown that 4-MBC intermediates exhibit acute toxicity.

1. Introduction

Pharmaceuticals and personal care products (PPCPs) comprise a diverse collection of thousands of chemical substances, including prescription and over-the-counter therapeutic drugs, veterinary drugs, fragrances, and cosmetics. Recent studies have shown that PPCPs considered to be emerging contaminants of environmental concern because of their continuous release into the aquatic environment, their persistence, and evidences for ecotoxicological effects [1].

Among them, sunscreen cosmetic products have been used for nearly 75 years and comprise substances (referred as UV filters) that are able to absorb UV radiation and protect human skin from direct exposure to the deleterious wavelengths of sunlight [2]. Studies have shown that UV filters may be accumulated in the aquatic environment through direct and indirect sources [2]. Direct input to natural waters stems from swimming and bathing (non-point sources) as well as industrial wastewater discharges (point sources) [3]. Indirect input, mostly related to wastewater discharge from wastewater-treatment plants (WWTPs), is also feasible, contributing to the accumulated burden in natural waters [4].

4-Methylbenzylidene camphor (4-MBC) is an organic camphor derivative that is used in the cosmetic industry (mostly used in sunscreen lotions and deodorants) for its ability to protect the skin against UV, specifically UV-B radiation. Studies have raised the issue that 4-MBC exhibits endocrine disrupting activity [5].

Concentration levels reported in the aqueous environment (<2–82 ng/L) fluctuate significantly as a function of sample location, size of the system under study (e.g., lakes and swimming pools), and type of recreational activities [6]. Analysis of domestic sewage in various WWTPs across Switzerland revealed concentrations in the range 560–6500 ng/L for 4-MBC, while elimination of 56% was observed in the effluent of the same municipal WWTPs, reaching concentration levels between 200 and 2700 ng/L [2].

4-MBC seems to be chemically stable and not readily biodegradable [2] while recent studies suggest that dissolved organic matter, nitrate and chloride play an important role in its photochemical elimination in natural waters [7].

4-MBC undergoes rapid photochemical isomerization [8,9]. Both isomers may be chiral and may comprise optical isomers (enantiomers), which exhibit identical physico-chemical properties, but which may differ in their biological behavior and effects [6].

* Corresponding author. Tel.: +39 0116707626; fax: +39 0116707615.
E-mail address: paola.calza@unito.it (P. Calza).

0926-3373/$ – see front matter © 2009 Elsevier B.V. All rights reserved.
doi:10.1016/j.apcatb.2009.04.013

Because surface water is the most affected, PPCPs may first pose a problem to utilities that use surface water as a source for drinking water production. Therefore, a crucial need for more enhanced technologies that can reduce their presence in the environment has become evident. In the last few years, new technologies for the decomposition of organic micro-pollutants in the aqueous environment have been developed. Heterogeneous photocatalysis [9,10] represents an example of advanced oxidation processes (AOPs) capable of achieving a complete oxidation of organic and inorganic species, including endocrine disrupting chemicals (EDCs) and pharmaceuticals as well as PPCPs [11–16].

To the best of our knowledge this is the first time that an extensive study of the photocatalyzed transformation of the UV filter 4-MBC is studied. The main objectives of this research were to assess the degradation of the pollutant in several different aspects.

Central composite design (CCD) based on response surface methodology (RSM) was employed to verify the interaction effects of factors responsible (TiO_2, H_2O_2 and light intensity) on the degradation efficiency of the pollutant. Besides, the application of desirability function for optimization of the photocatalytic process was employed in order to develop an efficient method for achieving maximum degradation efficiency of 4-MBC.

Another aspect of this work was the identification of possible intermediate products. For this reason powerful analytical techniques such as liquid chromatography coupled to mass spectrometry was employed. Moreover, in order to evaluate the toxicity of the irradiated solutions a bacterial assay was carried out based on the bioluminescence reduction of the marine bacterium *Vibrio fischeri*, using a Microtox Analyzer.

2. Experimental

2.1. Material and reagents

4-Methylbenzylidene camphor purity higher than 99% was a kind offer from Merck (Darmstadt, Germany). Solvents used: water and acetonitrile (HPLC grade) were obtained from Merck. Analytically pure grade hydrogen peroxide (30%), used in the experiments was from Merck (Darmstadt, Germany). Experiments were carried out using TiO_2 Degussa P25 as the photocatalyst. In order to avoid possible interference from ions adsorbed on the photocatalyst, the TiO_2 powder was irradiated and washed with distilled water until no signal due to chloride, sulphate or sodium ions could be detected by ion chromatography.

2.2. Irradiation procedures

Irradiation experiments of 4-MBC were carried out on stirred aqueous solutions contained in a cylindrical quartz glass UV-reactor. Degradations were performed on 50 ml of aqueous 4-MBC solutions with varying initial concentrations of TiO_2, H_2O_2 and different light intensities, according to the experimental design (Table 1). Before irradiation, the suspensions were allowed to stay in the dark for 60 min under stirring, to reach adsorption equilibrium on the semiconductor surface. Irradiation was carried out using a Suntest CPS+ apparatus from Heraeus (Hanau, Germany) equipped with a xenon arc lamp (1500 W) and special glass filters restricting the transmission of wavelengths below 290 nm. Chamber and black panel temperature were regulated by pressurized air cooling circuit and monitored using thermo-couples supplied by the manufacturer. The temperature of samples did not exceed 20 °C using tap water cooling circuit for the UV-reactor. To remove TiO_2 particles the solution samples were passed through 0.45 μm HA cellulose acetate membrane filters and were further analyzed by the appropriate analytical technique.

Experiments on intermediates have been performed in air saturated conditions using a 1500 W xenon lamp (Solarbox, CO.FO.MEGRA, Milan, Italy) simulating AM1 solar light and equipped with a 340 nm cut-off filter. The irradiation was carried out on 50 ml of suspension containing 0.4 mg/L 4-MBC and 50 mg/L TiO_2. The samples are then concentrated to 1 ml in a Bruket lyophilizer and injected into an HPLC/MS instrument.

2.3. Analytical procedures

2.3.1. Liquid chromatography

In the experiments where kinetic studies have been performed, during illumination of the aqueous solution, samples were withdrawn from the reactor at specific time intervals. The aqueous

Table 1
Central composite experimental design and results for 4-MBC degradation.

TiO_2–x_1 (mg/L)	H_2O_2–x_2 (mM)	Light intensity–x_3 (W/m^2)	$Degradation_{(exp)}$ (%)	$Degradation_{(calc)}$ (%)
−1	−1	−1	51.87	52.33
+1	−1	−1	63.34	64.74
−1	+1	−1	45.61	49.27
+1	+1	−1	67.36	66.91
−1	−1	+1	62.39	64.99
+1	−1	+1	73.74	72.24
−1	+1	+1	66.01	66.77
+1	+1	+1	77.56	79.25
0	0	0	73.20	73.97
0	0	0	74.76	73.97
0	0	0	73.44	73.97
(−α)	0	0	53.12	49.71
(+α)	0	0	70.27	70.63
0	(−α)	0	65.27	64.55
0	(+α)	0	70.20	67.97
0	0	(−α)	60.39	58.41
0	0	(+α)	80.51	79.44

			Levels
768	47.86	735	(+α, +1.68)
432	4.14	465	(−α, −1.68)
700	39.00	680	(+1)
500	13.00	520	(−1)
600	26.00	600	0

samples were filtered through 0.45 μm Millipore disks to remove TiO_2 particles and were extracted with SPE [17].

The LC system comprised a Shimadzu on-line DGU-14A degassing system coupled to an FCV-10AL controller unit and a LC-10AD high-pressure solvent delivery pump, with a 20 μl sample loop injector and a Shimadzu SPD-M10A UV/diode-array detector. The column material was a Discovery C_{18} (Supelco), with 5 μm particles (25 cm × 4.6 mm I.D.) with a guard column of the same material (8 mm × 3 mm). The column temperature was maintained at 30 °C. Water/acetonitrile (20/80%, v/v) was used for the isocratic elution of the analyte. Spectrum identification was performed at the absorbance maximum attained at the wavelength of 300 nm.

For the intermediates study, the chromatographic separations followed by a MS analyzer were run on a C18 column Phenomenex Synergi 4u-Fusion, 150 × 2.0 mm. Injection volume was 20 μL and flow rate 200 μL/min. Gradient mobile phase composition was adopted: 5/95 to 100/0 in 25 min acetonitrile/formic acid 0.05% in water.

2.3.2. Mass spectrometry

An LTQ Orbitrap mass spectrometer (ThermoFisher) equipped with an atmospheric pressure interface and an ESI ion source was used. The LC column effluent was delivered into the ion source using nitrogen as sheath and auxiliary gas. The source voltage was set at the 4.1 kV value. The heated capillary value was maintained at 275 °C. The acquisition method used was previously optimized in the tuning sections for the parent compound (capillary, magnetic lenses and collimating octapoles voltages) in order to achieve the maximum sensitivity. Mass spectra were collected in full scan positive mode in the range 50–500 m/z and in the tandem MS mode with collision energy (CE) generally chosen to maintain about 10% of the precursor ion. High resolution mass assignments were done with ±10 mmu accuracy.

2.3.3. Toxicity measurements

The toxicity of an unirradiated 4-MBC solution and of aqueous samples collected at different irradiation times, was examined by Microtox Model 500 Toxicity Analyzer; toxicity was evaluated by monitoring changes in the natural emission of the luminescent bacteria *V. fischeri* when challenged with toxic compounds. Freeze-dried bacteria, reconstitution solution, diluent (2% NaCl) and an adjustment solution (non-toxic 22% sodium chloride) were obtained from Azur. Samples were tested in a medium containing 2% sodium chloride, in five dilutions and luminescence was recorded after 5 and 15 min of incubation at 15 °C. Inhibition of the luminescence, compared with a toxic-free control to give the percentage of inhibition, was calculated following the established protocol using the Microtox calculation program.

2.3.4. Total organic carbon analyzer

Total organic carbon (TOC) was measured on filtered suspensions using a Shimadzu TOC-5000 analyzer (catalytic oxidation on Pt at 680 °C). The calibration was performed using standards of potassium phthalate.

2.4. Response surface methodology and experimental design

Response surface methodology is a collection of statistical and mathematical techniques useful for developing, improving and optimizing processes [18]. Besides the evaluation of relations existing between a group of controlled experimental factors and the observed results (of one or more selected criteria), RSM can derive a model that represents the whole process. Therefore, the application of statistical experimental design techniques in the development of the photocatalytic process can result in improved degradation efficiencies, reduced process variability combined with the requirement of less resources (time, reagents, and experimental work) [19].

At first, two-level fractional factorial design (resolution III) with five factors was used in order to eliminate unimportant factors before investing time and money in a more elaborate experiment. Five factors: pH, light intensity, 4-MBC concentration, TiO_2 and H_2O_2 concentrations were chosen, according to our previous experience dealing on the photocatalytic processes of micropollutants [11,12,15]. From the analysis of data (data not shown) only light intensity, TiO_2 and H_2O_2 have significant impact ($p < 0.05$) on 4-MBC degradation. The curvature was also significant, indicating that a higher order model or response surface study is needed in order to uncover the behavior of the significant factors. The CCD [20] was applied to investigate the simultaneous effect of TiO_2, H_2O_2 and light intensity in the photocatalytic degradation process as well as to evaluate the interactions between the three variables. For this design, 17 experiments were performed, at which the three variables (TiO_2, H_2O_2 and light intensity) were codified in five levels with three central points (Table 1).

The equation used to quantitatively describe the system and draw the response surface was built using STATISTICA® software, based on the experimental data obtained from 4-MBC degradation% after 15 min of irradiation during the photocatalytic treatment procedure.

2.5. Desirability function

Desirability function is a popular and established technique to concurrently determine these settings of input variables that can give the optimum performance levels for one or more responses. Harrington [21] first developed the desirability function, and it was later modified by Derringer and Suich [22] for specifying the relationship between predicted responses on a dependent variable and the desirability of the responses, a procedure that provides for up to three "inflection" points in the function. The desirability procedure involves three steps: (1) predicting responses on the dependent variable by fitting the observed responses using an equation, based on the levels of the independent variables, (2) finding the levels of the independent variables that simultaneously produce the most desirable predicted responses on the dependent variables and (3) maximize the overall desirability with respect to the controllable factors. Therefore, the main advantages of using desirability functions are to obtain qualitative and quantitative responses by the simple and quick transformation of different responses to one measurement.

Firstly, the response (U) is converted into a particular desirability function (df_i) that varies from 0 to 1. The desirability 1 is for maximum and desirability 0 is for non-desirable situations or minimum. Derringer and Suich [22] proposed the equation as:

$$df_i = \left(\frac{U-\alpha}{\beta-\alpha}\right)^{wi}, \quad \alpha \le U \le \beta \tag{1}$$

$$df_i = 1, \quad U > \beta$$
$$df_i = 0, \quad U < \alpha$$

In Eq. (1), α and β are the lowest and the highest values respectively, obtained for the response i, and wi is the weight.

The individual desirability scores for the predicted values for each dependent variable are then combined into overall desirability function, DF, by computing their geometric mean of different df_i values.

$$DF = [df_1^{v1} \times df_2^{v2} \times \cdots \times df_n]^{1/n}, \quad 0 \le v_i \le 1 \,(i = 1, 2 \ldots n), \quad \sum_{i=1}^{n} v_i = 1 \tag{2}$$

where df_i indicate the desirability of the response U_i (i = 1, 2, 3, ..., n) and v_i represents the importance of responses. Inspecting the desirability profiles, it determines which levels of the predictor variables produce the most desirable predicted responses on the dependent variables.

3. Results and discussion

3.1. 4-MBC stability and photolysis

Preliminary experiments were carried out, before the development of the experimental design, to evaluate the extent of hydrolysis and photolysis processes on the 4-MBC transformation. Results obtained from the adsorption in the dark, hydrolysis as well as direct photolysis for a time period of 90 min showed that the above abiotic processes were scarcely responsible for the observed fast transformations when the solution was irradiated in the presence of the TiO_2/H_2O_2 system.

3.2. Kinetics of disappearance

Several experimental results indicated that the degradation rates of photocatalytic oxidation of various organic contaminants over illuminated TiO_2 fitted the Langmuir–Hinshelwood kinetics model:

$$-r = \frac{dC}{dt} = \frac{kKC}{1 + KC}$$

where r is the oxidation rate of the reactant, C the concentration of the reactant, t the illumination time, k the reaction rate constant and K is the adsorption coefficient of the reactant. Taking into consideration the recent point of discussion with regards to L–H kinetics of photocatalytic reactions [23,24], for the development of multivariate approach, the efficiency of the photocatalytic procedure was evaluated as the degradation% after 15 min of light irradiation (Table 1, fourth column).

3.2.1. Response surface methodology

TiO_2 (x_1), H_2O_2 (x_2) and light intensity (x_3) were the input variables in order to get the degradation efficiency% (response) of 4-MBC. The complete design matrix (experimental conditions), range, levels of factors and the results obtained, are summarized in Table 1. The fourth column in Table 1 presents the experimental values obtained for the response factor (Y) and the fifth column the calculated values by way of the modeling procedure.

The sufficiency of the model was evaluated through analysis of variance (ANOVA). Moreover, Lack of Fit (LOF, i.e., the variation of the data around the fitted model) was also checked. In the present study with regards to 4-MBC degradation%, the LOF is not significant relative to the pure error, indicating good response to the model. The model regression coefficient (R^2) of 0.9639 is reasonable agreement with the experimental results, indicating 96.39% of the variability can be revealed by the model and is left with 3.61% residual variability.

The final mathematical equation in terms of significant coded factors for 4-MBC degradation% determined by STATISTICA software is given below:

$$\begin{aligned} Y = {} & 73.97(\pm 0.48) + 6.22(\pm 0.23)x_1 + 0.99(\pm 0.23)x_2 \\ & + 6.25(\pm 0.23)x_3 - 4.88(\pm 0.25)x_1^2 - 2.74(\pm 0.25)x_2^2 \\ & - 1.78(\pm 0.25)x_3^2 + 1.31(\pm 0.30)x_1x_2 - 1.29(\pm 0.30)x_1x_3 \end{aligned} \quad (3)$$

This mathematical expression (Eq. (3)) represents the response factor that is given by the percentage of 4-MBC degradation obtained from the decrease of its concentration after 15 min of photocatalytic reaction.

The variables x_1, x_2 and x_3 are TiO_2, H_2O_2 concentration and light intensity, respectively. The coefficients of the quadratic model in the equations were calculated by least-square multilinear regression analysis. The importance of each variable, depends on its signs and values as well as on the relative error (absolute value) associated with each value, which is indicated in parenthesis of Eq. (3). A coefficient is considered high when the associated relative error is lower than its value and low when its relative error is higher than its absolute value. Positive coefficients indicate that degradation is favored in the presence of high concentrations of the respective variables within the range studied, while negative coefficients indicate that the reaction is favored in the presence of low concentrations. Positive quadratic coefficients of x_1x_2 variables indicate a synergistic effect, while negative coefficients of x_1x_3 variables, an antagonistic effect between the variables.

Pareto analysis is a technique that helps to prioritize and focus resources visually, and to sort out which effect exerts a significant influence. As it can be seen (Fig. 1), the most important parameters of the overall treatment procedure were the light flux intensity followed by TiO_2 concentration, whereas H_2O_2 affect the degradation of the pollutant to a lesser extent. The efficiency of degradation was also affected slightly but significant (for the confidence level selected 95%), by two interrelated variables such as two factor interactions TiO_2/H_2O_2 (x_1x_2) and TiO_2/light intensity (x_1x_3).

Analyzing Eq. (3) and taking into consideration only the first-order effect, the optimum conditions for the photocatalytic degradation of 4-MBC seemed to be when TiO_2 (x_1) and light intensity (x_3) have a high value, since the highest numerical value of 4-MBC degradation (Y) corresponds to such conditions. Moreover, it seems that both variants affect likely the photocatalytic degradation of 4-MBC displaying a high coefficient. On the other hand, a slight positive effect with regards to the degradation efficiency could be associated with H_2O_2 concentration if we consider the first-order effect.

Nevertheless, an excess of TiO_2 (x_1), H_2O_2 (x_2) concentration and light intensity (x_3) in the system is adverse for the reaction, producing a negative influence on the photocatalytic performance (4-MBC degradation% decreased). The negative coefficients of quadratic terms x_1^2, x_2^2 and x_3^2 (as shown by the second-order effect) in the polynomial expression accounts for this effect. Besides, statistically significant interaction effects between the x_1x_2 and x_1x_3 variables were also observed.

The overall interaction effects are displayed in Fig. 2; a 3-D representation of the polynomial (Eq. (3)) obtained from the experimental data. The coordinates of the graph show the TiO_2 and H_2O_2 concentration (Fig. 2a), and TiO_2 and light intensity (Fig. 2b),

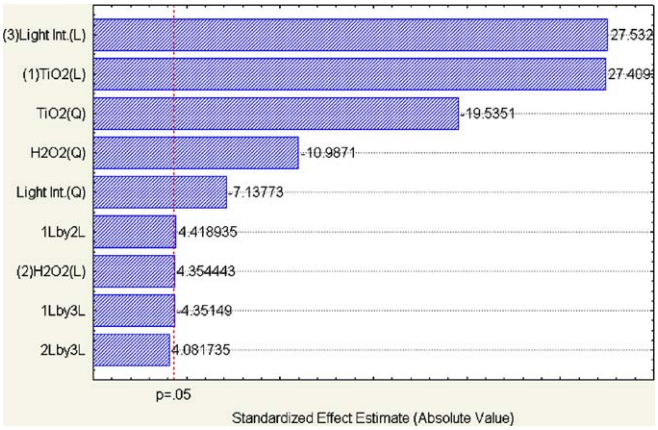

Fig. 1. Pareto chart of standardized effects of the main effects for 4-MBC degradation%. The vertical dashed line indicated the level of significance at p = 0.05.

respectively. The vertical axis represents the 4-MBC degradation% after 15 min of light irradiation during the photocatalytic process.

As shown in Fig. 2a the degradation rate increases proportionally to TiO_2 concentration (up to 550 mg/L), as expected, confirming the positive influence of the increased number of TiO_2 active sites on the process kinetics. At higher catalyst loading a decrease of 4-MBC degradation% was observed, irrespectively of the initial H_2O_2 concentration. The availability of active sites increases with catalyst loading, but the light penetration, and hence, the photoactivated volume of the suspension shrinks. Similar observations have also been reported in other studies on various organic substances [25,26]. In addition, the decrease on the degradation rate at higher catalyst loading may be due to deactivation of activated molecules by collision with ground state molecules [27].

It can be seen (Fig. 2a) that when the concentration of hydrogen peroxide increases, the degradation rate smoothly increases. This positive effect may be attributed to the inhibition of electron–hole recombination at the semiconductor surface by accepting a photogenerated electron from the conduction band and thus promoting the charge separation (Eq. (4)):

$$e_{CB}^- + H_2O_2 \rightarrow OH^- + {}^\bullet OH \quad (4)$$

The higher reaction rates with increasing H_2O_2 can also be attributed to the increase in the concentration of hydroxyl radicals. These radicals are generated by Eq. (4) while on the other hand, peroxide may be split photocatalytically to produce hydroxyl radical directly (Eq. (5)) or by reaction with superoxide anion (Eq. (6)) [28]:

$$H_2O_2 + h\nu \rightarrow 2{}^\bullet OH \quad (5)$$

$$H_2O_2 + O_2^- \rightarrow {}^\bullet OH + OH^- + O_2 \quad (6)$$

However, when high concentrations of H_2O_2 are used, the degradation% diminishes since it may act as $^\bullet OH$ scavenger [29] reducing the amount of radicals available to destroy the 4-MBC molecules (Eq. (7)).

$$H_2O_2 + {}^\bullet OH \rightarrow HO_2 + H_2O \quad (7)$$

Although other radicals are produced ($HO_2^\bullet$) their oxidation potential is much smaller than the $^\bullet OH$ species [30].

As already mentioned light intensity and TiO_2 display the strongest effects individually, with regards to the photocatalytic degradation of the target compound. If we consider their interaction (Fig. 2b), it can be seen that irrespective of titania loadings an increase of the light intensity increases the degradation of the pollutant. Moreover, its profile can be divided in two parts: in the beginning the degradation reaction seems to be proportional to the light intensity, thus confirming the photo-induced nature of the activation of the catalytic process, with the participation of photo-induced electrical charges (electrons and holes) to the reaction mechanism [31]. In other words the incident photons are efficiently converted into active species that act in the degradation of the target compound.

However, at higher values the rate varies as fractional order between zero and one [32]. This behavior is related to the significant negative quadratic effect of light intensity (x_3^2) and also the antagonist effect (x_1x_3) with TiO_2 concentrations which limit the efficiency of the process and slow down the reaction rate. These two effects originate mainly from the electron–hole recombination which becomes predominant [33] at the respective experimental conditions.

3.2.2. Optimization by desirability function

The profile for predicted values and desirability option in the STATISTICA® software is used for the optimization process. Profiling the desirability of responses, involves, first, specifying the desirability function for each dependent variable (degradation%), by assigning predicted values a scale ranging from 0 (undesirable) to 1 (very desirable).

The CCD design matrix results from Table 1, represented the maximum (80.51%) and minimum (45.61%) degradation% of 4-MBC. According to these values, desirability function settings for each dependent variable of 4-MBC degradation% are depicted at the right of Fig. 3: desirability of 1.0 was assigned for maximum degradation% (80.51%), 0.0 for minimum (45.61%) and 0.5 for middle (63.06%).

On the left hand side of Fig. 3 (bottom), the individual desirability scores are illustrated, respectively, for the photocatalytic efficiency of 4-MBC. Since desirability 1.0 was selected as the target value, the overall response (degradation%) obtained

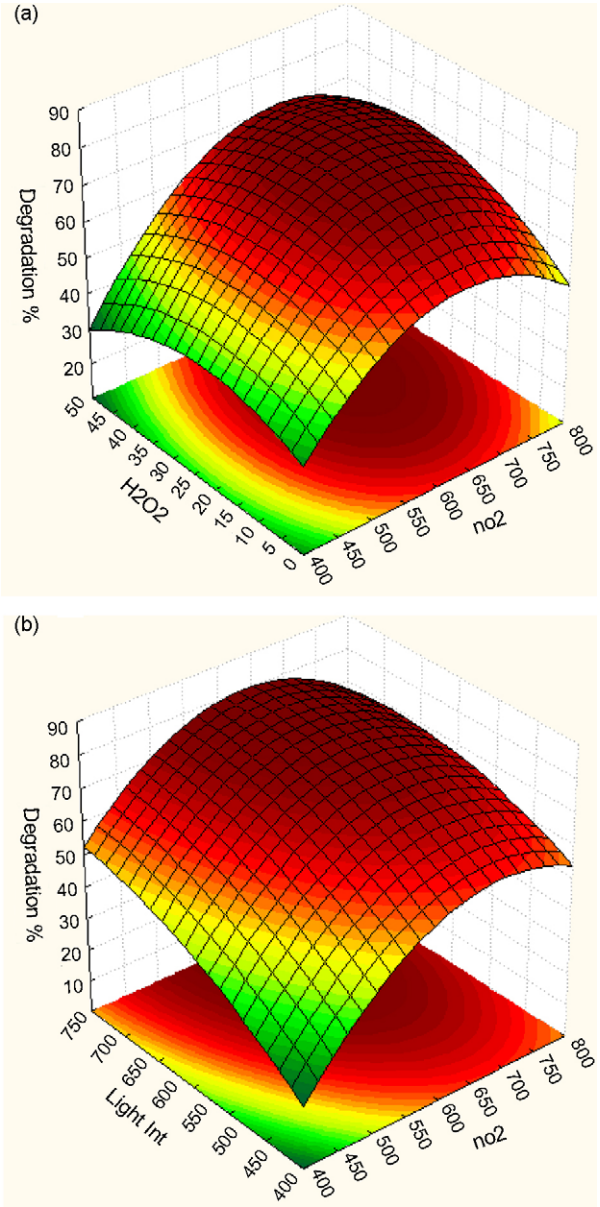

Fig. 2. Response surface showing the effect of (a) TiO_2 concentration and H_2O_2, (b) TiO_2 concentration and light intensity, on the degradation rate expressed as 4-MBC degradation% after 15 min irradiation.

from these plots with the current level of each factor in the model are depicted at the top (left) of Fig. 3. These figures allow seeing at a glance how changes in the level of each variable affect not only response (degradation%) but also overall desirability of the responses.

On the basis of these calculations and choosing desirability score of 1, software optimized 80.92% degradation of 4-MBC with calculating the optimized model variables of TiO_2 684 mg/L, H_2O_2 37 mM and 735 W/m^2 for light intensity.

Finally, for validation, duplicate assenting experiments were conducted using the optimized parameters. The results are closely co-related with the data obtained from desirabilty optimization analysis using CCD, indicating that CCD with desirability function could be effiectively used to optimize the photocatalytic degradation of the target analyte.

A usual requirement of an efficient catalytic reaction is its application, or in other words the ability of the optimized method to provide accurate and precise results despite variations in equipment and conditions. For this reason the target compound was tested at the optimal conditions found from RSM coupled to desirability function, in natural river water (pH 7.9, conductivity 311 μS/cm, total dissolved solids 218 mg/L, total organic carbon 4.53 mg/L). Results have shown that the response of interest (degradation efficiency) was not significantly influenced by changing the aqueous matrix from distilled to natural river water, demonstrating a degradation yield of 76% after 15 min of illumination.

3.3. Characterization of the 4-MBC decomposition products

The study of the 4-MBC transformation products was performed in the presence of TiO_2 50 mgL^{-1}. The complete disappearance of the initial compound occurs within 20 min of irradiation. Along with the disappearance of 4-MBC, five organic compounds characterized by different m/z ratio are formed, whose evolution profiles as a function of irradiation time are shown in Fig. 4. The intermediates were characterized by HPLC/HRMS taking into account their chromatographic behavior and kinetics of evolution, coupled with the exact mass information and the analysis, when available, of the MS^n spectra. Table 2 resumes all the formed compounds together with their MS^n peculiar losses.

Unsubstituted camphor MS^n spectra (see Table 2) and its transformation products (Table S1, additional material) were also analyzed, with the goal to enlighten the structural attribution through the investigation of the role of the aromatic system on the 4-MBC transformation. Looking closer to the camphor MS^2 spectra analysis, it afforded the detachment of water, ketene and propenol. Thus, the MS^2 fragmentation is confined to the 6-term ring, while the bridged moiety is preserved. Conversely, for 4-MBC the fragmentation still involves the camphor moiety of the structure, with the formation of the product ions at m/z 237.1608 (loss of water from the 4-MBC enolic form), 157.0992 (breaking up of the camphor moiety), 213.1251 (detachment of the bridged moiety) and 213.1614 (loss of ketene), so stressing that the bridged moiety is deeply involved in the MS^2 fragmentation. MS^n further fragmentation proceeds as described in Scheme 1.

The differences observed in the MS^2 spectra are still maintained in camphor and 4-MBC transformation products. While the camphor photocatalyzed transformation proceeds through the formation of hydroxy and aldheydic derivatives (see additional material), 4-MBC follows a more articulated transformation mechanism, that also involves the detachment of the bridged moiety.

A first 4-MBC transformation pathway (I) (Fig. 5) leads to the formation of a species labelled B, at $[M+H]^+$ 241.1527. Its empirical formula can be deduced from its exact mass and is

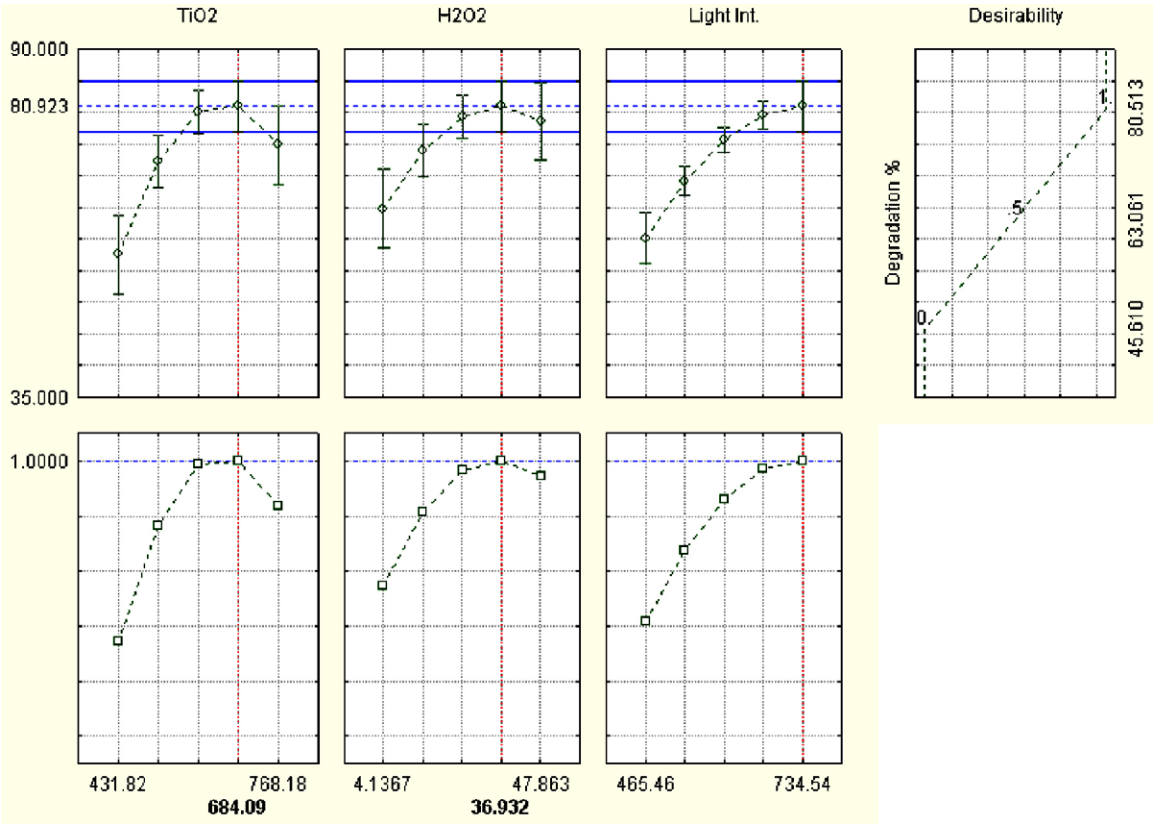

Fig. 3. Profiles for predicated values and desirability function for 4-MBC photocatalytic degradation%. Dashed line indicated current values after optimization.

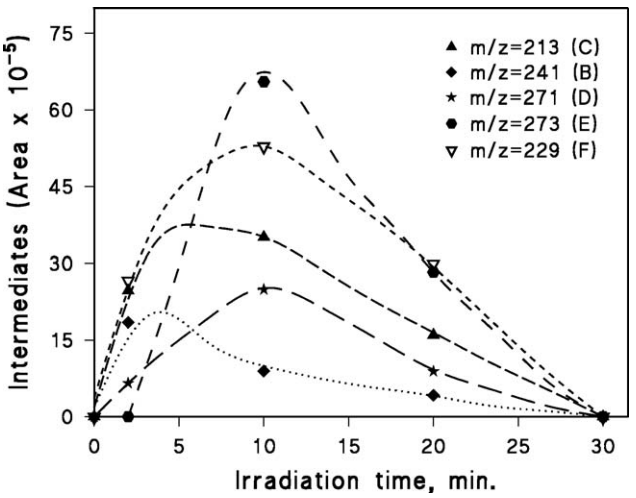

Fig. 4. Main intermediates generated from 4-MBC degradation through an initial oxido/reductive sequence.

attributed to the 4-MBC demethylated derivative. Unfortunately, no peculiar MS^2 products are formed, so that the available information do not permit to assess which of the methyl groups is involved. We suggest that demethylation occurs on the camphor moiety.

A second photocatalyzed transformation route (II) leads to the formation of two species at higher molecular weight: $[M + H]^+$ 271.1885, labelled D and $[M + H]^+$ 273.1678 (E) attributed to the hydroxy and bihydroxy/demethylated 4-MBC derivatives, respectively. The hydroxylation in D seems to involve a methyl group. These considerations are supported by MS^n analysis that shows, on one side, the product ion at m/z 240.2320 (loss of the CH_3O radical), while a concomitant fragmentation route leads to the product ion at m/z 253.3046, through the loss of a water molecule. The noticeable reduction in the retention time from A to D suggests as preferential point of attack the methyl located on the aromatic ring. The formation of benzyl alcohol from toluene during photocatalytic treatment is documented [34] and supports the supposed structure. D is probably transformed into the species E, through a demethylation/hydroxylation combination.

E is the less retained compound and eliminates two water molecules, so stressing the entrance of a second hydroxyl group, that should be reasonably located on the camphor moiety. The entry of a second hydroxyl group induces a moderate reduction in the retention time, in agreement with the involvement of the camphor moiety. The occurrence of hydroxylation on 5- or 6-position is reported via bacterial attack on the camphor structure [35] and should also similarly occur under photocatayltic treatment.

A third transformation pathway (III) leads to the formation of the compound C. The stable species C at $[M + H]^+$ 213.1415 should share the same structure proposed for the 4-MBC MS^2 product ion of composition $C_{15}H_{17}O$ (see pathway III); unfortunately MS^n analysis could not support the hypothesis because of an interference due to background signals. The detachment of the bridged moiety should be induced by an oxido/reductive sequence that involves a concerted attack by an OH/e^- pair, followed by the elimination of water and the formation of a double bond that enlarges the conjugated system.

For the intermediate compound at $[M + H]^+$ 229.1411, labelled F, the empirical formula can be deduced from its exact mass. It is reasonably formed though the detachment of the bridged moiety and the entrance of a hydroxyl group. Taking into account the temporal profiles, this intermediate compound could be formed from the species B. The marked reduction in the retention time from C to F suggests that hydroxylation should again involve the methyl of the benzyl moiety.

Even if all the identified compounds are degraded themselves within 30 min, the complete carbon mineralization is only achieved after 24 h of irradiation (see Figure S1, supplementar material).

3.4. Toxicity evaluation

Several aqueous samples at different irradiation times were analyzed to estimate the percentage of inhibition of each sample and the data are collected in Fig. 6. The initial toxicity of 4-MBC solution (0.2 mg L^{-1}, 0 h of irradiation-distilled water) showed an inhibition of 16%. The toxicity profile shows a slight increase of the toxicity solution in the early steps of the photocatalytic process. Since the disappearance of 4-MBC is complete within 20 min of irradiation, the measured toxicity should be attributed to the formation of toxic intermediate compounds. Even if a correlation between the intermediates formed and the toxicity can be seen, it was not possible to assess which molecule is responsible of the

Table 2
List of main $[M + H]^+$ and fragments coming from MS and MS^n spectra obtained from 4-MBC and its intermediate compounds.

	$[M + H]^+$	Empirical formula	t_R (min)	Product ions	
				MS^2	MS^3
A	255.1748	$C_{18}H_{22}O$	34.15	237.1608 ($-H_2O$) [100]	195.1146 ($-C_3H_6$) [100] 209.1301 ($-C_2H_4$) [48] 181.0990 ($-C_4H_8$) [25]
				157.0992 ($-C_6H_{10}O$) [50]	142.0759 ($-CH_3$) [100]
				213.1251 ($-C_3H_6$) [34]	195.1147 ($-H_2O$)
				213.1614 ($-C_2H_2O$) [14]	
				199.1089 ($-C_4H_8$) [27]	157.0994 ($-C_2H_2O$)
Camphor	153.1255	$C_{10}H_{17}O$		135.1125 ($-H_2O$) [100]	107.0837 ($-C_2H_4$) [100] 93.0681($-C_3H_6$) [32]
				109.0994 ($-C_2H_4O$) [79]	–
				95.0839 ($-C_3H_6O$) [59]	–
B	241.1527	$C_{17}H_{20}O$	23.55	–	–
C	213.1415	$C_{15}H_{16}O$	20.15	–	–
D	271.1885	$C_{18}H_{22}O_2$	13.63	253.1939 ($-H_2O$) [85]	–
				240.2320 ($-CH_3O$) [100]	–
E	273.1678	$C_{17}H_{20}O_3$	8.19	237.1127 ($-2H_2O$) [100]	–
F	229.1411	$C_{15}H_{16}O_2$	9.48	–	–

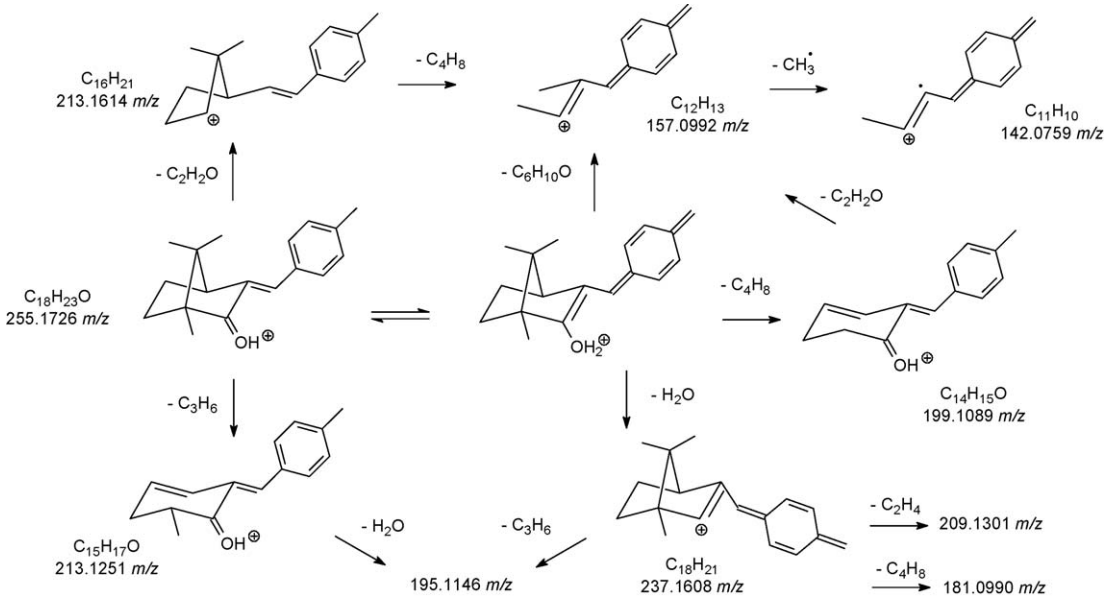

Scheme 1. Fragmentation pathway followed by 4-MBC.

toxicity. Moreover, the increase in the toxicity is moderate and could be affected by experimental uncertainty. However, looking closer to the temporal profiles shown in Fig. 4, only the species labelled C ($[M + H]^+$ 241.1527) reaches the highest concentration after 2 min and consequently the increased toxicity in the first steps of the photocatalytic treatment should be linked to its presence; conversely four species, labelled B ($[M + H]^+$ 213.1415), F ($[M + H]^+$ 229.1411), D ($[M + H]^+$ 271.1885) and E ($[M + H]^+$ 273.1678), show their higher intensities after 10 min of irradiation. From 15 min to 16 h of irradiation the inhibition percentage decreases, but remains still high if compared with 4-MBC initial toxicity. Since after 30 min of irradiation all the identified compounds are completely disappeared, the measured toxicity should be linked to the formation of secondary transformation products. A final value of less than 1% is only reached after 24 h of irradiation.

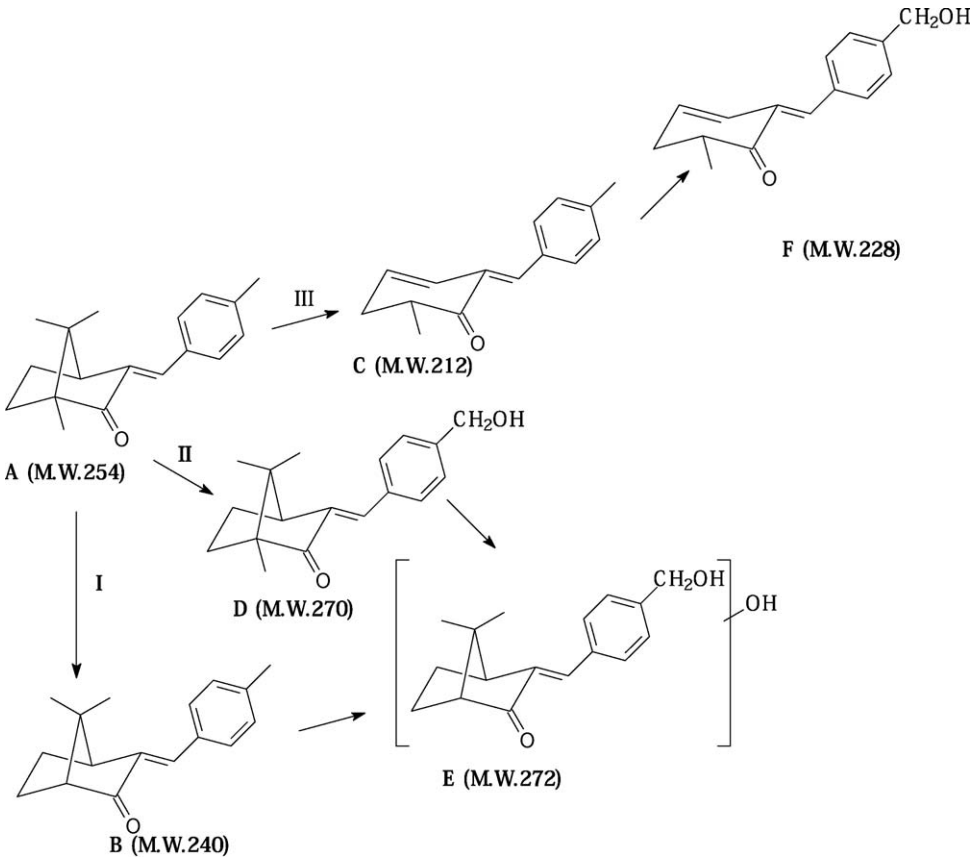

Fig. 5. Possible transformation pathways followed by 4-MBC under photocatalytic treatment.

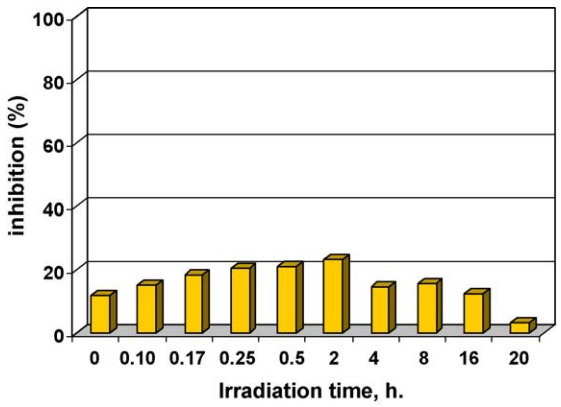

Fig. 6. Inhibition (%) of the luminescence of bacteria *Vibrio fischeri* as a function of the photocatalytic treatment time.

4. Conclusions

The analytical utility of multivariate chemometric techniques in the investigation of 4-MBC photocatalyzed degradation has been demonstrated. RSM was applied fruitfully for predicting the model and to establish the relationships between the variables (TiO_2, H_2O_2 and light intensity) that affect 4-MBC degradation%. Moreover, desirability function was used to identify optimum degradation efficiency% by calculating specific factors optimization simultaneously. By using CCD with desirability function, 80.92% degradation of 4-MBC, is possible within the studied parameter levels.

4-MBC was transformed under photocatalytic treatment into several species. The degradation compounds were identified by means of HRMS and toxicity evaluation showed a relationship with the initial concentration of these products. Methylbenzylidine moiety was involved into hydroxylation or demethylation reaction, while the camphor moiety is subjected to progressive demethylation, with the final detachment of the bridged moiety.

Acknowledgements

This research was financially supported by the project PENED (03ED926), of the Greek General Secretariat of Research and Technology. Financial support by Universita' di Torino - Ricerca Locale is also gratefully acknowledged. Prof. Glauco Tonachini and Dr. Giovanni Ghigo are kindly acknowledged for the stimulating discussions.

Appendix A. Supplementary data

Supplementary data associated with this article can be found, in the online version, at doi:10.1016/j.apcatb.2009.04.013.

References

[1] V.L. Cunningham, M. Buzby, T. Hutchinson, F. Mastrocco, N. Parke, N. Roden, Environ. Sci. Technol. 40 (2006) 3456–3462.
[2] D.L. Giokas, A. Salvador, A. Chisvert, TrAC Trends Anal. Chem. 26 (2007) 360–374.
[3] C.G. Daughton, T.A. Ternes, Environ. Health Perspect. 107 (1999) 907–938.
[4] T. Poiger, H.R. Buser, M.E. Balmer, P.A. Bergqvist, M.D. Muller, Chemosphere 55 (2004) 951–963.
[5] A. Klann, G. Levy, I. Lutz, C. Muller, W. Kloas, J.P. Hildebrandt, Environ. Res. 97 (2005) 274–281.
[6] M. Silvia Diaz-Cruz, M. Llorca, D. Barcelo, TrAC Trends Anal. Chem. 27 (2008) 873–887.
[7] D.L. Giokas, A.G. Vlessidis, Talanta 71 (2007) 288–295.
[8] H.R. Buser, M.D. Muller, M.E. Balmer, T. Poiger, I.J. Buerge, Environ. Sci. Technol. 39 (2005) 3013–3019.
[9] P. Schneider, A. Bringhen, H. Gonzenbach, Drug Cosmet. Ind. 159 (1996) 32–38.
[10] A. Fujishima, K. Hashimoto, T. Watanabe, TiO_2 Photocatalysis: Fundamentals and Applications, BKC Inc., Tokyo, 1999.
[11] P. Calza, V.A. Sakkas, C. Medana, C. Baiocchi, A. Dimou, E. Pelizzetti, T. Albanis, Appl. Catal. B: Environ. 67 (2006) 197–205.
[12] P. Calza, V.A. Sakkas, A. Villioti, C. Massolino, V. Boti, E. Pelizzetti, T. Albanis, Appl. Catal. B: Environ. 84 (2008) 379–388.
[13] S. Esplugas, D.M. Bila, L.G.T. Krause, M. Dezotti, J. Hazard. Mater. 149 (2007) 631–642.
[14] J.M. Herrmann, J. Disdier, P. Pichat, S. Malato, J. Blanco, Appl. Catal. B: Environ. 17 (1998) 15–23.
[15] V.A. Sakkas, P. Calza, C. Medana, A.E. Villioti, C. Baiocchi, E. Pelizzetti, T. Albanis, Appl. Catal. B: Environ. 77 (2007) 135–144.
[16] C. Zwiener, F.H. Frimmel, Water Res. 34 (2000) 1881–1885.
[17] D.L. Giokas, V.A. Sakkas, T.A. Albanis, J. Chromatogr. A 1026 (2004) 289–293.
[18] R.H. Myers, D.C. Montgomery, Process and Product Optimization Using Designed Experiments, 2nd ed., Wiley Interscience, New York, USA, 2002.
[19] U.K. Garg, M.P. Kaur, V.K. Garg, D. Sud, Bioresour. Technol. 99 (2008) 1325–1331.
[20] G.E.P. Box, W.G. Hunter, J.S. Hunter, Data Anal. Model Building (1978).
[21] E.C. Harrington, Ind. Qual. Control 21 (1965) 494–498.
[22] G. Derringer, R. Suich, J. Qual. Technol. 12 (1980) 214–219.
[23] A.V. Emeline, V.K. Ryabchuk, N. Serpone, J. Phys. Chem. B 109 (2005) 18515–18521.
[24] D.F. Ollis, J. Phys. Chem. B 109 (2005) 2439–2444.
[25] K. Nohara, H. Hidaka, E. Pelizzetti, N. Serpone, J. Photochem. Photobiol. A: Chem. 102 (1997) 265–272.
[26] C.M. So, M.Y. Cheng, J.C. Yu, P.K. Wong, Chemosphere 46 (2002) 905–912.
[27] K. Nohara, H. Hidaka, E. Pelizzetti, N. Serpone, Catal. Lett. 36 (1996) 115–118.
[28] A. Duran, J.M. Monteagudo, Water Res. 41 (2007) 690–698.
[29] J.M. Monteagudo, M. Carmona, A. Duran, Chemosphere 60 (2005) 1103–1110.
[30] J.H. Ramirez, C.A. Costa, L.M. Madeira, Catal. Today 107–108 (2005) 68–76.
[31] J.M. Herrmann, Catal. Today 53 (1999) 115–129.
[32] D.F. Ollis, E. Pelizzetti, N. Serpone, Environ. Sci. Technol. 25 (1991) 1523–1529.
[33] M. Sleiman, D. Vildozo, C. Ferronato, J.M. Chovelon, Appl. Catal. B: Environ. 77 (2007) 1–11.
[34] C. Minero, V. Maurino, E. Pelizzetti, Mar. Chem. 58 (1997) 361–372.
[35] R.W. Eaton, P. Sandusky, Appl. Environ. Microbiol. 75 (2009) 583–588.